Photon beamline diagnostics

S. Hustache-Ottini
Synchrotron SOLEIL, Saint Aubin, France

1 Introduction

Synchrotron radiation sources deliver photon beams over a very wide energy spectrum and with high brilliance, for many different fields of application from biology, chemistry, micro- and nano-electronics to pharmacology, cultural heritage, etc. Every beamline (or BL) is a singular experiment (sometimes even several experiments), and on one beamline there are different ways to prepare the photon beam for the users, depending on the scientific goal. The consequence for photon beam diagnostics is that there are so many. Therefore, this lecture does not intend to give an exhaustive overview of photon beam diagnostics but rather to give an idea of the variety of the possible diagnoses and of what can be done at a third-generation synchrotron radiation facility with different kinds of techniques.

I chose to exploit only examples which are or will be in operation at SOLEIL. This is of course restrictive, but still representative if one considers that SOLEIL beamlines cover the electromagnetic spectrum from far infrared (THz) to hard X-rays (tens of keV) as can be seen on Fig. 1 (more details can be found on the SOLEIL website: http://www.synchrotron-soleil.fr/).

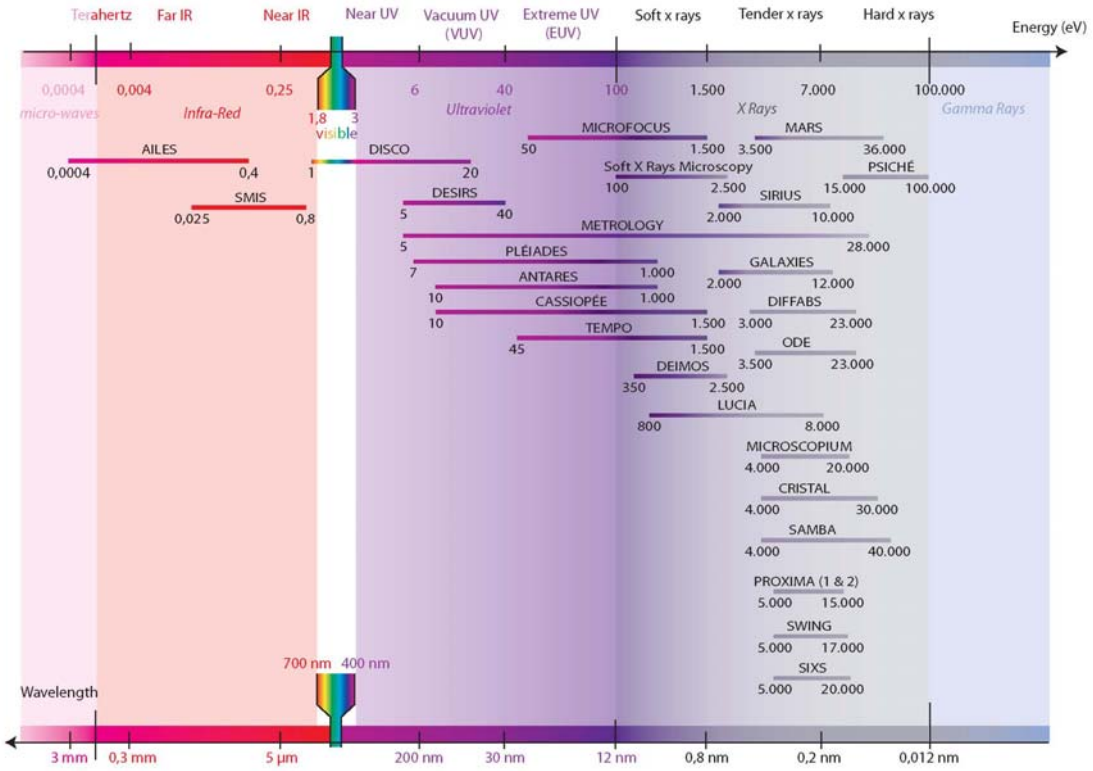

Fig. 1: Breakdown of SOLEIL beamlines according to photon energy (top) or wavelength (bottom)

Nevertheless, a drastic selection had to be made, and many techniques will not even be mentioned. The criteria for the selection aimed to show the diversity of the detectors, ranging from commercial ones to 'in-house' designed devices, from the cheapest to the more sophisticated and costly ones.

To understand why the devices are so miscellaneous, it is necessary to know how a beamline is built, what are the main elements acting on the photon beam, and which kind of parameters have to be measured. The first part of this lecture is therefore dedicated to the general description of two beamlines standing on each end of the energy range of SOLEIL. It points out some particular features of the beamline which have consequences for the diagnostics.

The second part shows that the diagnoses are divided into three families, namely the measurement of the photon beam position, the imaging function, and the determination of the number of photons or intensity. A few examples are given for each of these families and an original design developed at SOLEIL is described in more detail in the third part.

2 What is a synchrotron beamline made of?

In this section, a basic description of two beamlines will help to understand why there are so many different ways to diagnose the photon beam, depending on the energy range or on the scientific goal and the techniques of the experiment. The first subsection describes the front end, which has functions common to all the beamlines. The second and third subsections are dedicated to a high- and a low-energy beamline and present the different components which are usually present.

2.1 The front end

The first section of a beamline is called the front end and is located in the storage ring tunnel. Figure 2 shows the example of a beamline of SOLEIL on a bending magnet, but regardless of the light source of the BL (bending magnet or insertion device), the functions of this front end are:

- to stop the photon beam, in case for instance of a maintenance of the beamline downstream. This is done by an occulter (see Fig. 2)
- to reduce the power transmitted down to what is necessary to achieve the scientific goal of the BL and consequently to protect the optics located downstream. The 'extra light' is stopped by the fix absorber (see Fig. 2) and on the undulator BL by an additional adjustable diaphragm. This aperture is of the order of a fraction of mrad, horizontally and vertically, i.e., of the order of 1 mm at 10 m. This implies (as well as the previous function of the occulter) the absorption and dissipation of a strong power. It can reach 5 kW on a soft X-ray BL on HU80, or even 21 kW on the future in-vacuum wiggler BL Psiché. But it is not only the power but the power density which can be very high and reach 300 W/mm^2 at 10 m from the source on the in-vacuum undulators U20 BL. Finally, only a few per cent of this power is transmitted to the beamline.
- to ensure the vacuum safety of the storage ring, with an 'acoustic delay line' which delays the pressure wave in case of an incident along the BL and provides enough time for a fast valve to close.
- to participate in radiation safety with a γ-ray trap which is designed to stop a large fraction of the bremsstrahlung photons coming from the storage ring. This trap is closed during the electron beam injections.
- to perform the first diagnosis on the photon beam. On the example of Fig. 2, two X-ray Beam Position Monitors (XBPM) determine two positions of the centre of gravity of the photon beam, giving an indication of the angle of emission. A more detailed description of this kind of device is given in Section 3.

The typical size of these components and the complexity of their task imply that one of the first diagnoses to be performed after the wall of the storage ring tunnel is to check that the transmission of the beam through the front end is good and that there are no obstacles along its path.

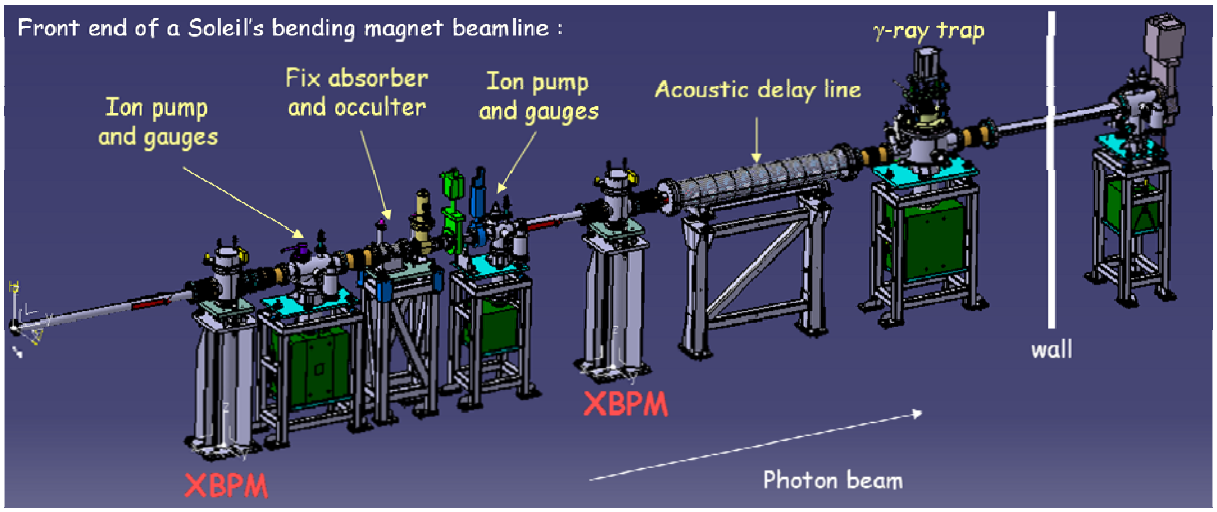

Fig. 2: 3D view of the front end of a SOLEIL beamline whose light source is a bending magnet in the storage ring

2.2 A hard X-ray beamline: Cristal

Cristal is specialized in X-ray scattering, or more precisely, diffraction which is one of the most powerful methods of obtaining information on the atomic structure of matter. The light source of the BL is an in-vacuum undulator U20, delivering photons in the 4–30 keV energy range. A schema of the BL is shown in Fig. 3.

The length of the photon path, from the source down to the experiment position is 35 m. Since the photons here are hard X-rays, the entire beamline is enclosed in hutches made of lead for radiation safety reasons. All the devices, including photon beam diagnostics, have to be remotely controlled and cannot be accessed during operation.

The first hutch, on the right of Fig. 3, the so-called optics hutch, contains the monochromator which selects in the white beam a single photon energy in a narrow bandwidth. The optics hutch can also host one or several mirrors used for focusing purposes. On Cristal, there are three end stations (or experiments), located in two different experimental hutches and which cannot be used at the same time. There are therefore three focusing distances, selected thanks to the mirrors. Each end station is equipped with a diffractometer, a device with several circles (up to six in this case) to orientate the sample and the detectors with respect to the beam. To avoid parasitic scattering on air, the beam is propagated in pipes under moderate vacuum but the diffractometers and therefore the samples and detectors for the experiment are in air.

All the equipment and the progress of the experiments are followed from the control room, located behind the last experimental hutch (on the left of Fig. 3).

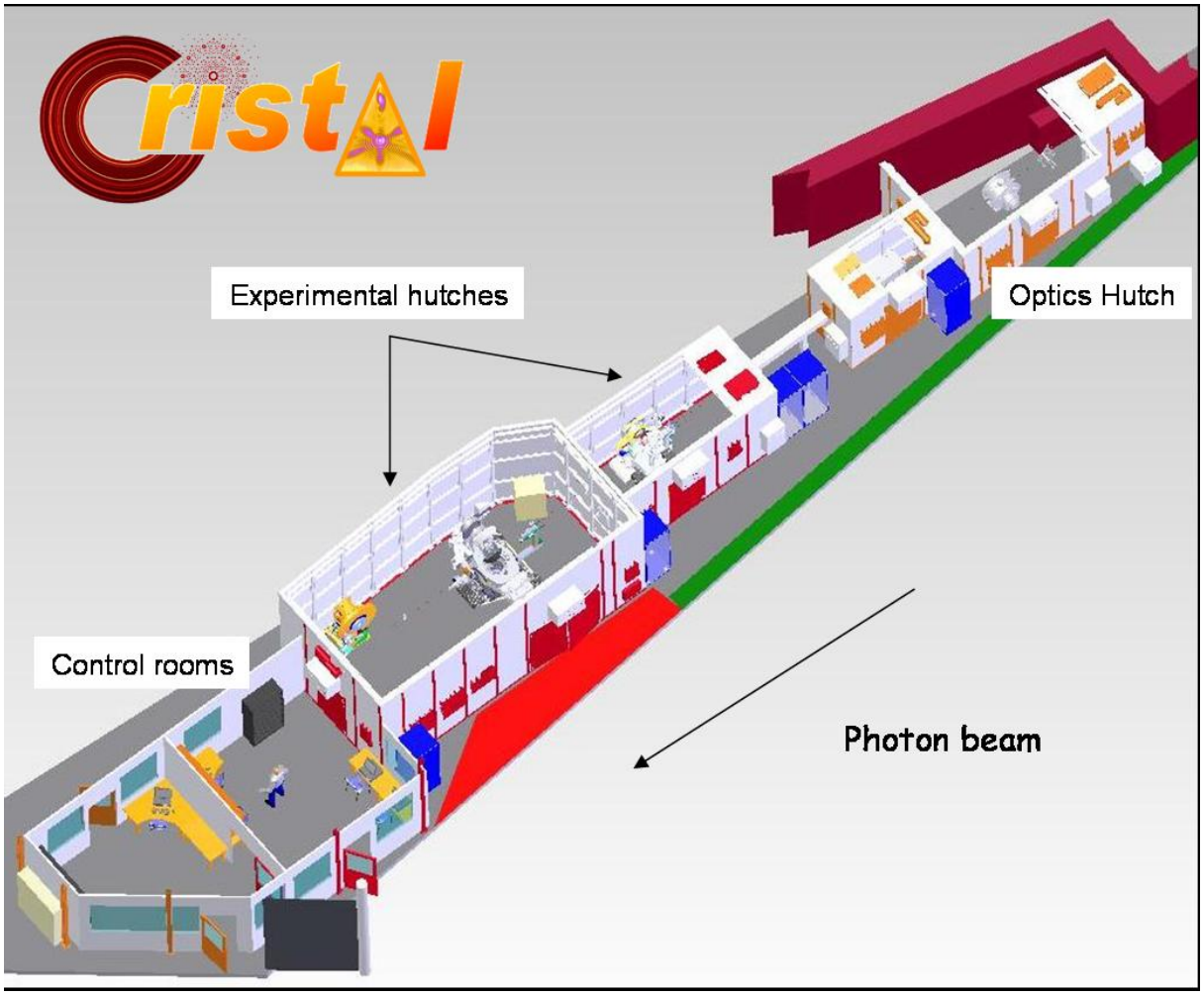

Fig. 3: 3D view of the Cristal beamline, from the optics hutch down to the control rooms

2.3 A vacuum ultraviolet (VUV) beamline: Désirs

Désirs is dedicated to the study of photon-induced processes via the valence shell on dilute samples such as cold molecules, radicals, and laser-excited species. It is a high-resolution spectroscopy BL, which furthermore makes use of the polarization properties (linear and circular) of the light emitted by the undulator HU640. The energy range achievable with this source is 5–40 eV, and as a consequence, all the beamline, including the sample and the detection set-ups, are under ultra-high vacuum. The total length from the source down to the sample can be as long as 63 m.

Since the low-energy photons are absorbed by the walls of the vacuum pipes, only the first mirror of the BL is inside a lead hutch, as can be seen on Fig. 4. The other components (monochromator, mirrors, end stations, diagnostics, etc.) stand directly in the experimental hall of SOLEIL. Visual and manual control are therefore possible.

There are also three end stations on this BL (one on white beam, two on monochromatic beam), but contrary to Cristal, they are distributed over three branches, fed with the beam by deviation mirrors.

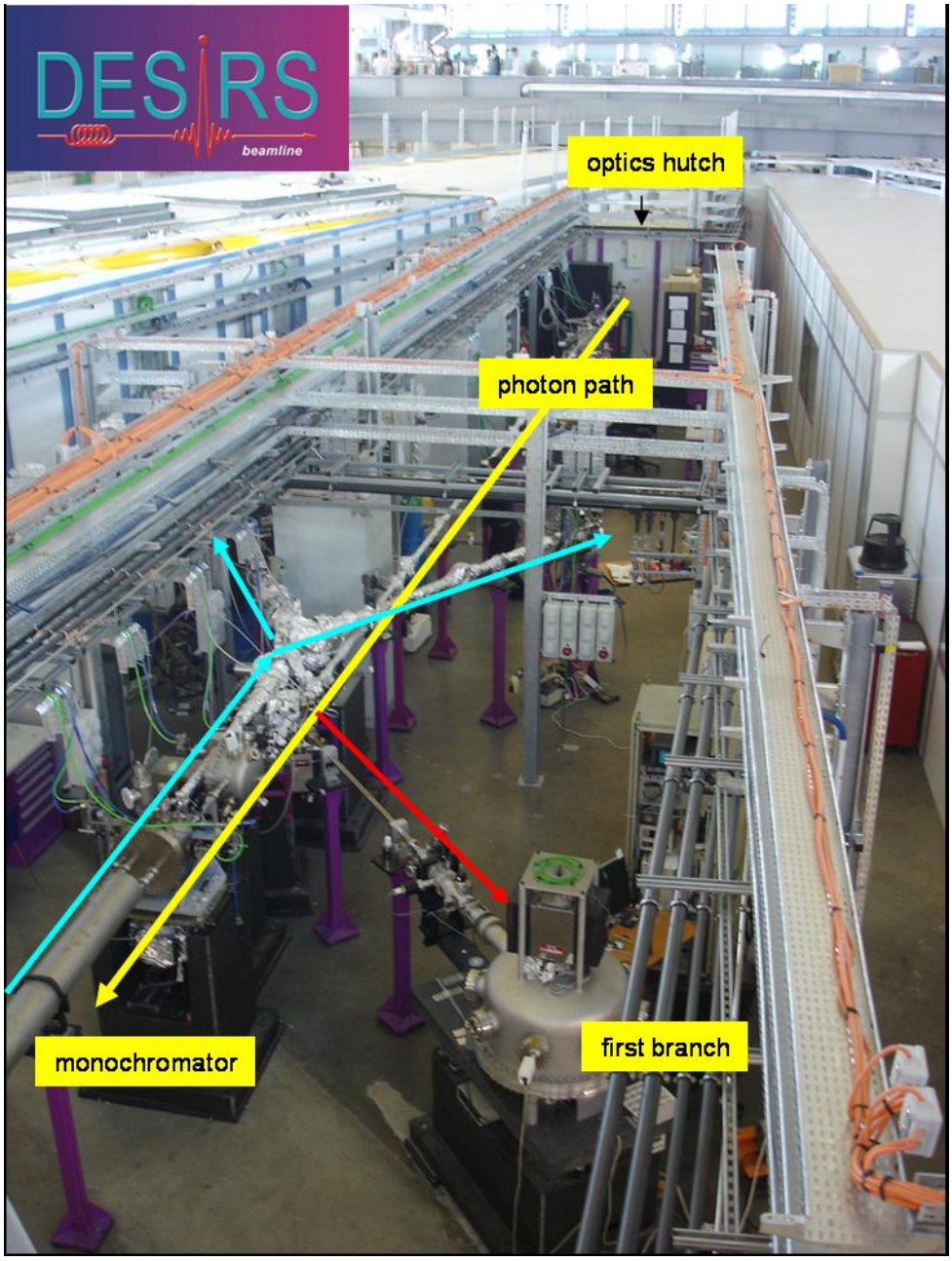

Fig. 4: Photograph of the Désirs beamline in the experimental hall of SOLEIL. The photon beam comes from the top, through the optics hutch. It can be deviated towards the first branch (red arrow) or the monochromator from which the photons go back to the second or third branch (light blue arrows).

2.4 Summary

The different components of a typical beamline were presented above. Since the path of the photons is several tens of metres and the beam is subjected by these components to major transformations along this path, one can easily understand that a lot of parameters have to be checked on the propagation axis.

In the front end, the photons are emitted and the global shape of the beam is defined, with a constraint of high power absorption and dissipation. It is, at this point, necessary to verify that there is

no unforeseen obstacle, that the absorbers are correctly aligned and for BL on insertion device, it is important to determine the position and the inclination of the optical axis (which depend on the alignment of the undulator with respect to the electron beam) along which the optics downstream will be aligned. The front end is also a good place to check for the electron beam stability through the photon beam stability, before increasing the complexity of the analysis with the mirrors and monochromators. These measurements can be correlated to the electron beam diagnostics.

Along the beamline itself, the photon beam undergoes dramatic changes, induced by the optics: it can be deflected towards one or another branch; it can be focused (down to the tens of nanometres scale on some BL) at various distances; the energy of the photon is defined within a narrow band by the monochromators. After each of these operations, one needs to know whether the transmission is optimal, whether the beam is at the expected position and what is its shape (is it homogeneous, structured?). For spectroscopy BL, it is also important to measure the resolving power of the optics, i.e., the energy width of the monochromatic beam.

At the experiment, the studied sample has to be aligned with respect to the beam. For microscopy experiments, the maximum focusing point has to be found by observing the dimensions of the beam, down to the µm scale (even below on future BL of SOLEIL). During the experiment, the stability of the beam has to be at the same scale and the on-line measurement of the position of the beam can be used for feedback on the optics. And finally, the ‘on-line’ measurement of the incoming photon flux is needed for normalization purposes for almost any kind of experiment. This flux measurement may also be used for feedback to compensate for thermal drifts or low-frequency vibrations of the mirrors.

To summarize, from the source down to the sample, and depending on the experiment, it is necessary to visualize the beam, to locate it, and to determine its intensity in various environments (air, primary vacuum, ultra-high vacuum, with high power density or low flux), without disturbing the beam if the information is needed on-line, to various degrees of precision.

3 The main functions in photon beam diagnosis

As was shown in the previous section, there are three main kinds of data to be determined to drive the photon beam from the light source in the storage ring to the sample, several tens of metres downstream: the position, the intensity, and the shape (or image) of the beam. There are many techniques and only a few of them will be enumerated in the following paragraphs. Examples of several methods employed at SOLEIL at various positions of different beamlines are developed in more detail, together with the results obtained.

3.1 Position of the photon beam

Table 1 lists (not exhaustively) some examples of techniques commonly used at synchrotron beamlines for the measurement of the position of the beam.

The first column identifies the technique and the stars indicate that examples will be developed in Sections 3.1.1 and 3.1.2, the second one gives the energy range of photons where this technique is usually employed (but this distribution is not ‘strict’). In the third column, a distinction is made between techniques giving the real position of the beam as opposed to an apparent position. For the latter case, the detector is in contact with only a fraction of the photons and therefore the method makes the assumption that the photon distribution is regular and symmetric. By contrast, when the detector is in contact with the entire envelope of the beam, the result is the true position of the barycentre of the incoming photons.

And finally, the method may be direct (measurement of the photons of the beam themselves) or indirect (measurement of a phenomenon induced by the photons such as fluorescence): the consequence is sometimes a weaker signal in the latter case and therefore degraded performance.

It should be noted that, most of the time, the position is not measured on an event-by-event basis but relies on the measurement of the photocurrent generated by the photons and on reconstruction of a centre of gravity or barycentre.

Table 1: Examples of techniques commonly used at synchrotron sources for the measurement of the beam position

Technique	Usual energy range	Type of measurement
*Photo-ionization on metals + barycentre (on a useless part of the beam)	All	Apparent position / Direct
Wire scan (photo-ionization)	All	Real position / Direct
*Position-sensitive semiconductor (e.g. silicon or diamond) + barycentre	All	Real position / Direct
Ionization chambers	Hard X-rays	Real position / Direct
Detection of beam-induced fluorescence or scattering + barycentre	Hard X-rays	Real position / Indirect

The first two methods, by generating a photocurrent on metal electrodes standing out of the useful beam or on a metallic wire scanned across the beam, can be used during the experiment since they do not or only weakly intercept the photons. The wire scan gives the position in only one direction.

Semiconductor detectors, made out of silicon or diamond for instance, may be position sensitive with a dedicated electrode structure. They may be thinned enough (down to a few μm) to be semi-transparent in the hard X-ray energy range (above 5 keV) and be used in parallel with the experiment. For lower energies, they are mainly used during the settings of the BL. Ion chambers are often limited to hard X-rays because of the windows for gas confinement.

For the last method, a very thin foil (down to ~1 μm) of an appropriate material (i.e., adapted to the working energy; it can be aluminium, Kapton, etc.) is inserted in the path of the photons. The scattered or fluorescence photons emitted are detected by four photodiodes for instance. The coordinates of the centre of the beam are those of the barycentres of the signals.

In the following paragraphs, examples of photo-ionization on metal and of position-sensitive semiconductors are detailed for two applications on opposite ends of the energy range of SOLEIL.

3.1.1 Example 1: X-ray beam position monitors in the front end of BL on insertion device

SOLEIL beamlines on insertion devices are equipped in the front end with one or two X-ray Beam Position Monitors (XBPM) manufactured by the company FMB [1]. The aim of these detectors is to perform an early diagnosis of the photon beam, very close to the light source, which will be correlated to the electron BPM data and will be used for stability checking.

Photographs of a device are displayed in Fig. 5. Figure 5(a) shows the four very tiny tungsten blades which intercept the white beam outside of the region useful for the beamline. The spacing of the blades is a few mm. Figure 5(b) is a picture of an XBPM installed in a front end of Bessy [2]. The

image in Fig. 5(c) shows how the blades of the XBPMs upstream and downstream are shifted, to avoid the screening of the second XBPM by the first.

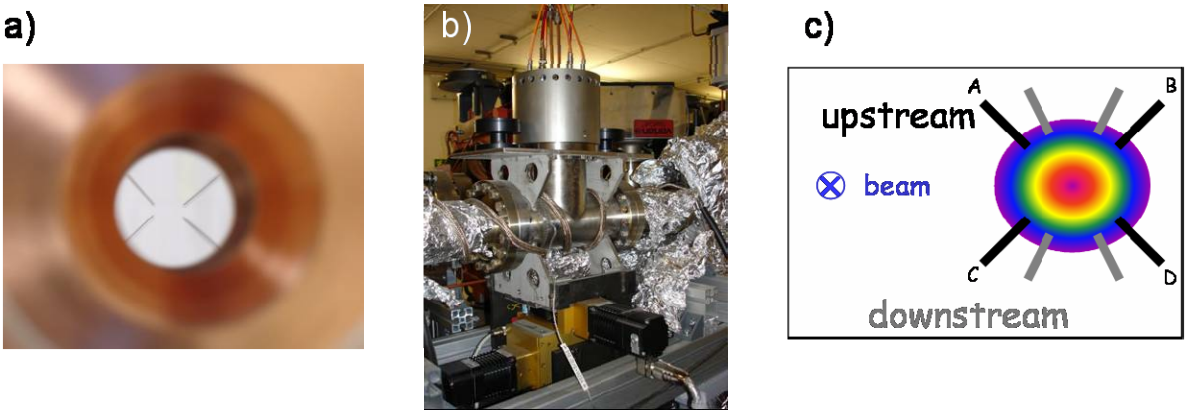

Fig. 5: (a) Photograph of the four tungsten blades of an XBPM. (b) Photograph of an XBPM installed in a front end at Bessy. (c) Diagram of the position of the blades of the XBPM located upstream (black), of the blades of the XBPM located downstream (grey) with respect to the white beam (rainbow).

The determination of the position in one direction relies on the asymmetry of the photocurrents induced on one pair of blades with respect to the opposite pair. For instance, the vertical position z for one XBPM is given by:

$$z \propto \frac{(I_A + I_B) - (I_C + I_C)}{I_A + I_B + I_C + I_D}$$

where I_i are the photocurrents induced on the i^{th} electrode, the position of this electrode being defined in Fig. 5(c).

In 2001, Karsten Holldack [3, 4] demonstrated that these XBPMs, with their sub-µm resolution and their time response can be used for a local feedback on the vertical position, as shown in Fig. 6 from Ref. [3]. The upper part shows the readback and set values of a steerer as a function of time, with feedback on and off. The feedback is performed upon the values delivered by the XBPM located downstream and the effect is verified by looking at the position given by the XBPM located upstream (bottom of Fig. 6). The local orbit correction is very efficient, since, when feedback is on, the vertical position becomes stable within ±2 µm instead of ±4 µm with feedback off.

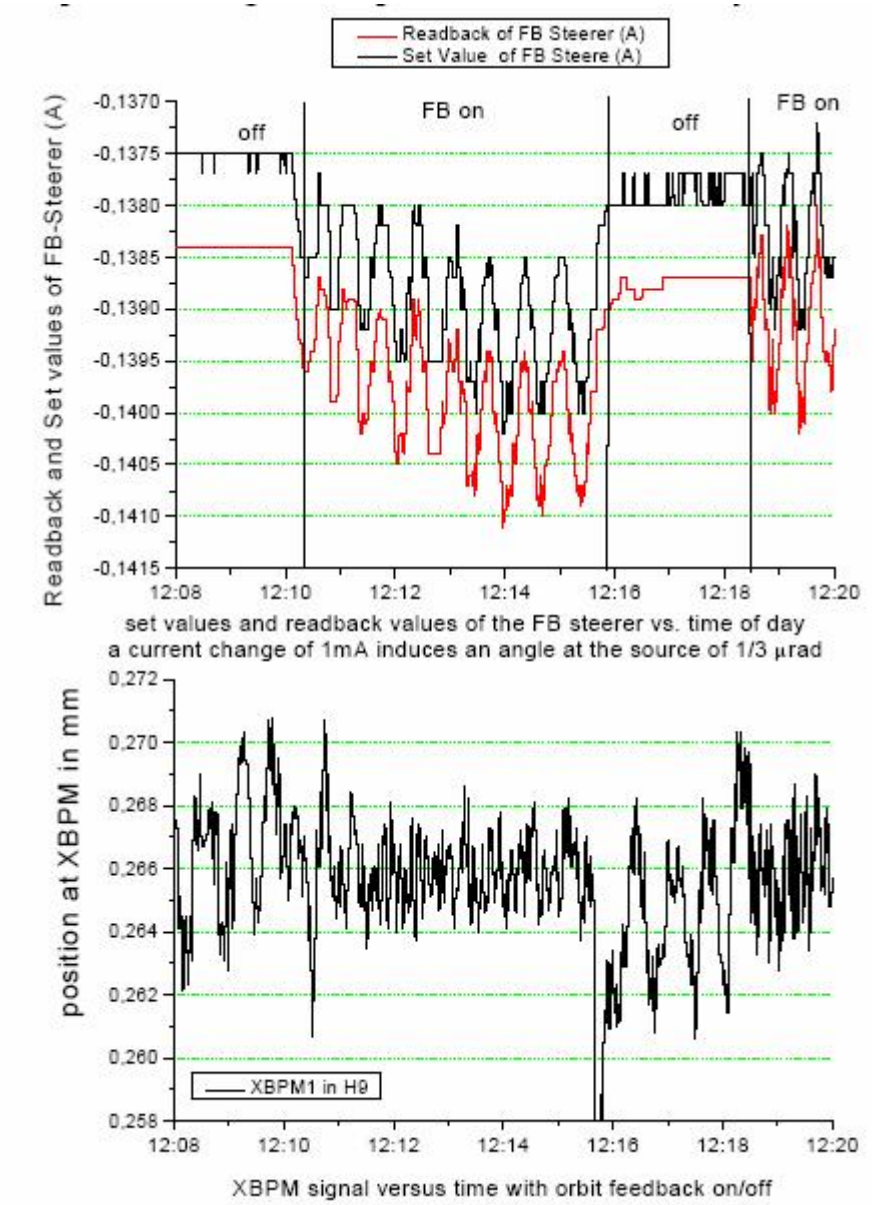

Fig. 6: From Ref. [3] "Local orbit feedback test at U49/1 using a closed loop realised with EPICS. The orbit was vertically corrected to the downstream XBPM 2 while the figure shows the upstream XBPM 1 signal control channel."

3.1.2 Example 2: Four-quadrant photodiode on Désirs

This second example for the measurement of the position of the photon beam is regularly used on the Désirs BL. The detector is a four-quadrant silicon photodiode procured from IRD [5]. The detector and the mechanical set-up employed on Désirs are shown on Figs. 7(a) and 7(b).

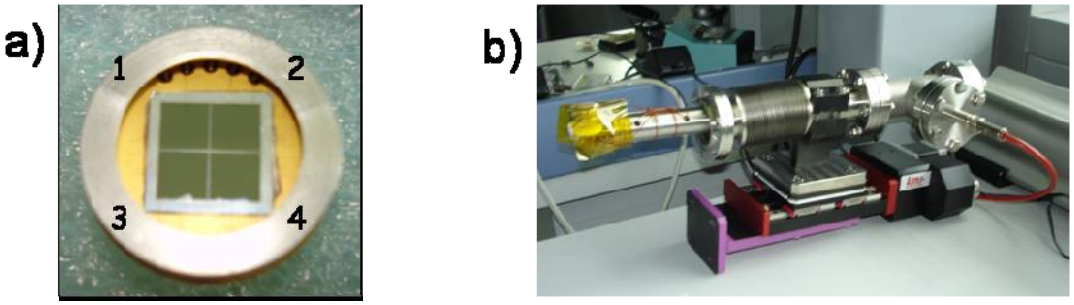

Fig. 7: (a) Photograph of the IRD photodiode [5], (b) photograph of the mechanical set-up for mounting on Désirs

The diagnostic is mounted in 'pink beam', before the monochromator but after a mirror whose reflectivity is low for the highest energies of the incoming white beam. The goal of the diagnosis is to adjust the vertical and horizontal movements of the second mirror M2 so that the beam is centred on the entrance of the so-called 'gas filter'. This device suppresses the higher orders in energy of the insertion device, and this operation is crucial for this high-resolution spectroscopy beamline, the experiments relying on the beam energy purity. The principle is to make the beam go through a gas where the photons of the highest energies, i.e., above an absorption threshold of the gas, are absorbed. The maximum energy on the beamline is 40 eV, and no window can be used for the confinement of the gas with respect to the ultra-high vacuum of the BL. The gas volume is insulated from the rest of the beamline by a sequence of very small 2 mm diameter capillaries, through which the beam must pass.

The centre of the photodiode is precisely aligned beforehand with the centre of the capillaries, whose horizontality is also adjusted. The setting of the mirror M2 before the experiment consists in moving it until a (0,0) position (i.e. barycentre of the beam in the centre of the detector) is measured by the photodiode. Figure 8 shows the coordinates of the centre of the photon beam during vertical and horizontal scans of M2 over the active area of the photodiode (5×5 mm^2), the sensitivity of the detector being a few tens of µm.

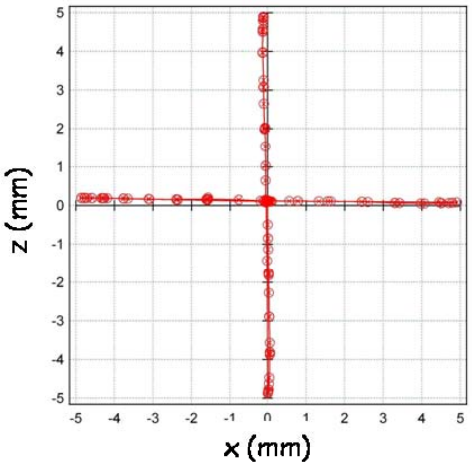

Fig. 8: Coordinates of the centre of gravity of the beam measured by the four-quadrant photodiode from IRD [5] during a scan of the horizontal and vertical movements of the mirror M2 on the Désirs BL. The sensitivity of the diagnostic is of a few tens of µm.

3.2 Imaging the photon beam

Taking a picture of the photon beam is a very powerful means of diagnosis. The basic idea is to convert the X-rays into visible light, but the choice of the converting fluorescent screen will depend on the power to be dissipated, the beam size, the resolution required, and the environment at the place of the diagnostic. The visible light is usually observed by a CCD camera with objective and lenses. The set-up also changes with the application, the magnification depending on the size of the beam which can go down to a few tens of nm. Figure 9 shows the different combinations in use today at SOLEIL.

The white beam on hard X-ray beamlines on insertion devices is small, a few hundreds of µm in the horizontal and vertical directions, the power and the power density are high, up to several hundred W/mm^2. The fluorescent screen chosen is artificial diamond, obtained by chemical vapour deposition CVD [Fig. 9(a)]. This material is very radiation hard and has a very high thermal conductivity (about five times higher than copper) to dissipate the incident power. The semi-transparent screen is placed in high vacuum. When excited by photons, it emits violet light which is observed in air through a viewport by a CCD camera with a dedicated objective.

For white beam of BL on bending magnet, we use the same principle but the beam is much larger and the power to be dissipated is still around a few hundred watts. In collaboration with Saint Gobain Solcera [6], SOLEIL developed a brazing technique to ensure a good thermal contact between a water-cooled copper holder and a (30 × 100 mm^2) alumina doped with Cr (AF995R or Chromox) screen [Fig. 9(b)].

To image the monochromatic beam, regardless of the light source, there is no more high power to evacuate and the choice of the screen mainly depends on the size of the beam and on the desired resolution. One of the most employed scintillators is yttrium aluminium garnet or YAG doped with cerium but new materials and new methods are continuously being investigated (see for instance Ref. [7]). On bending magnet BL [Fig. 9(c)], a polycrystalline YAG:Ce from Baikowski [8] is preferred because of the large size of the beam (30 × 100 mm^2), single-crystal YAG(Ce) being much more expensive in these dimensions.

The configuration used to image the monochromatic beam on a hard X-ray BL on an insertion device is shown on Fig. 9(d). By the use of a thin single crystal (100 µm) and by minimizing the working distance of the optics, the resolution is improved down to 10 µm, and thus to the beam size which is of the order of hundreds of µm.

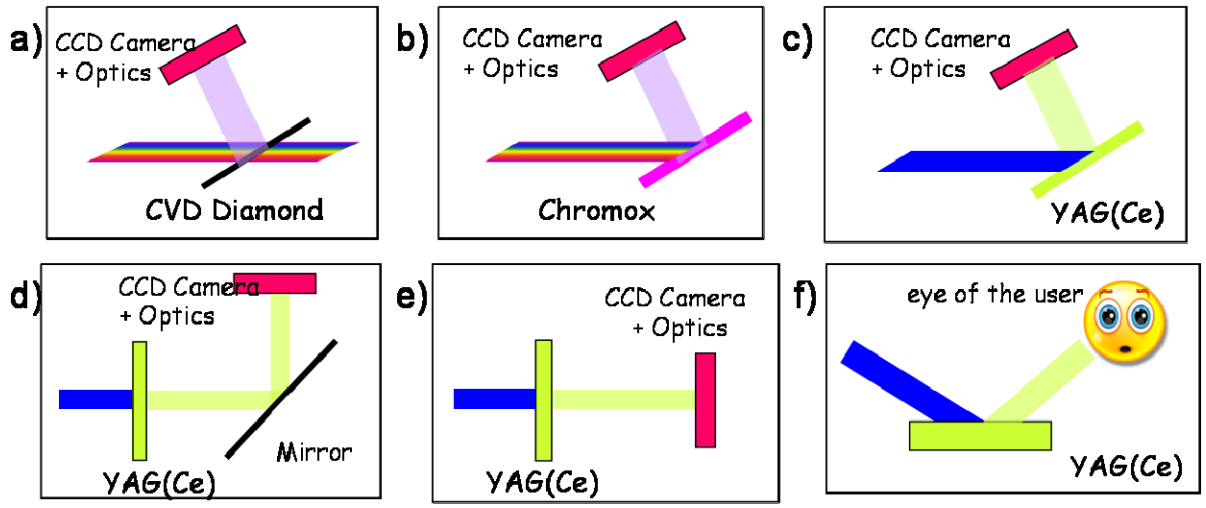

Fig. 9: Examples of the scintillators screen / optics combination used at SOLEIL for beam imaging. See text for comments

To check and improve the focusing of the beam at the sample level on hard X-ray beamlines, in air, SOLEIL also developed X-ray cameras based on the principle of Fig. 9(e), with various magnifications, from 0.5 to 10. And finally, on low-energy BL, since the vacuum pipes where the beam propagates can be approached during operation, a very powerful detector is often used: the eye of the user [Fig. 9(f)].

3.2.1 Example 1: Imaging the white beam

To get an image of the white beam is usually the first operation done on the beamline, on the opening day. With this image, the good transmission of the front end is verified and the basic parameters of the photon beam can be assessed. An example is shown on Fig.10, where the white beam imager based on CVD diamond was used to observe the very first undulator beam on Cristal. The transmission of the front end was good and the size of the beam was as expected.

The image of the pink beam (i.e., after the very first mirror, but still with a high power to dissipate) is also used to diagnose the optics themselves. Figure 11 shows two images of the beam after the first mirror of the bending magnet BL Samba, taken with the Chromox beam viewer. On the top image, small dots are clearly visible: they were identified to be gallium drops. This gallium is used to ensure the thermal contact between the silicon mirror and the cooling system. This material was not correctly deposited during the manufacturing and came to the surface of the mirror during pumping down. The image of the beam after the cleaning of the mirror is shown in the bottom of Fig. 11: the drops were suppressed and the mirror is operational.

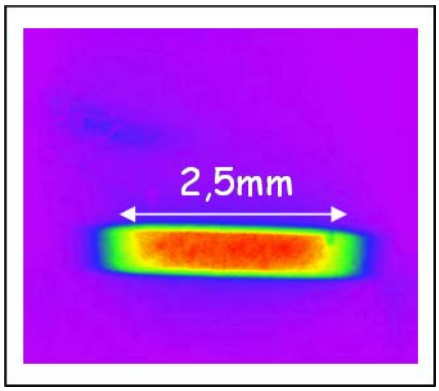

Fig. 10: First white beam observed with a CVD diamond-based imager on the opening of Cristal

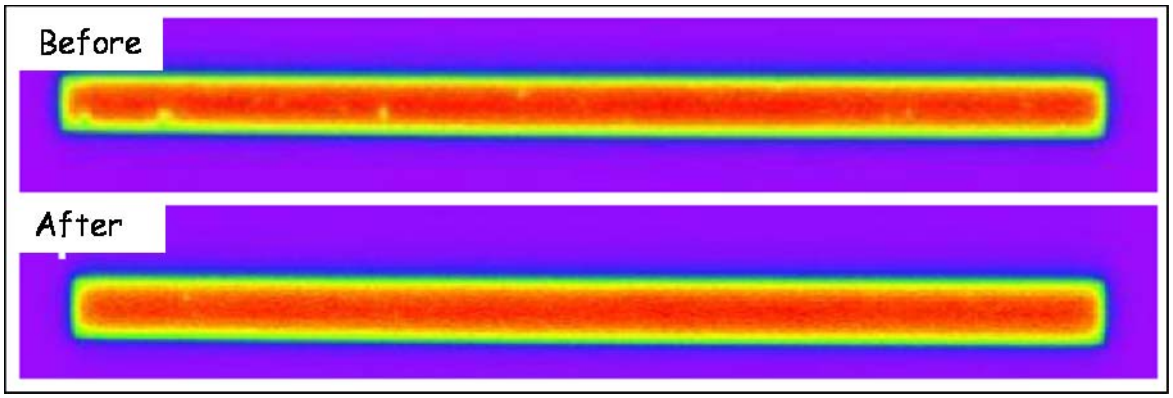

Fig. 11: Top: image of the pink beam (after the first mirror) on the bending magnet BL Samba. The surface of the mirror is contaminated with gallium drops. Bottom: same image after a cleaning of the surface of the mirror.

3.2.2 Example 2: Imaging the monochromatic beam

As for the pink beam, the monochromatic beam is usually observed after every transformation of the beam on the BL. There is often a beam viewer placed behind every optics and slits, which can, as mentioned in the previous paragraph, be diagnosed with the image obtained. The image is also used for alignment and focusing purposes, as can be seen on Fig. 12. This image was taken during the final set-up of an experiment, at the sample position with an X-ray camera in air. The sample to be studied is a small silicon ball (diameter: 350 µm) standing at the extremity of a borosilicate capillary and the aim of the diagnosis was to align this ball with the maximum intensity region of the 28 keV beam, before closing the last slits symmetrically around this position.

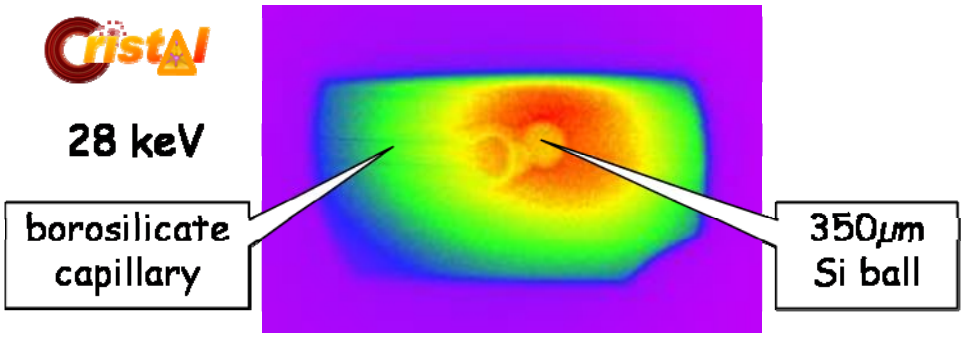

Fig. 12: Image of a silicon sample held by a borosilicate capillary during alignment set-up on Cristal. The image was taken with an X-ray camera (magnification: 0.5) and the energy of the photons was 28 keV.

3.3 Intensity of the photon beam

Table 2 lists (again not exhaustively) some examples of techniques commonly used at synchrotron beamlines for the measurement of the intensity of the photon beam.

The first column identifies the technique, the second one gives the energy range of photons where this technique is usually employed (but this distribution is not 'strict'). In the third column, the direct or indirect type of the technique is detailed. As in Section 3.1, it indicates whether the photons of the beam are directly detected or the scattered or fluorescence photons they induce are detected. The technique may be used 'in transmission', that is to say in parallel with the experiment: this is the case when intensity is determined for normalization purposes. The diagnostics stopping the beam completely (i.e., 'not in transmission') are, for instance, a measurement of the absolute flux of monoenergetic photons or the intensity measurement used for the energy calibration of the monochromator.

Table 2: Examples of techniques commonly used at synchrotron sources for the measurement of the beam intensity

Technique	Usual energy range	Type of measurement
Semiconductor (silicon or diamond)	All	Direct / In transmission or not for the lower energies
Photo-ionization on metal (gold) grids with high transparency (>80%)	VUV, soft X-rays	Direct / In transmission
Ionization chambers	All	Direct / In transmission or not for the lower energies
Detection of beam-induced fluorescence or scattering	Tender or hard X-rays	Indirect / In transmission

Semiconductors are widely used, and thin silicon photodiodes (down to 5 µm) recently appeared which are transparent enough to be used in transmission on hard X-ray BL. It is the case also for diamond whose stopping power for hard X-rays is much lower than silicon. As was mentioned in Section 3.1, this kind of device may become position sensitive with a suitable electrode structure.

Photo-ionization on metal grids is widely used at SOLEIL. The main difficulties are the handling of the very thin grid with high transparency and the measurement of low currents which can go down to the nA level or even below.

Ionization chambers are mainly used on hard X-ray beamlines, but also at lower energies for very special diagnosis such as the determination of the resolving power of a monochromator in the soft X-ray region (see for instance Ref. [9]).

As in Section 3.1, for the last method, a very thin foil (down to ~1 µm) of an appropriate material (i.e., adapted to the working energy; it can be aluminium, Kapton, etc.) is inserted in the path of the photons (see Fig. 13). The scattered or fluorescence photons emitted are detected by photodiodes or a scintillator and photomultiplier tube. The intensity is proportional to the number of detected photons. This method is preferred when the absorption of incoming photons has to be kept low (a few per cent).

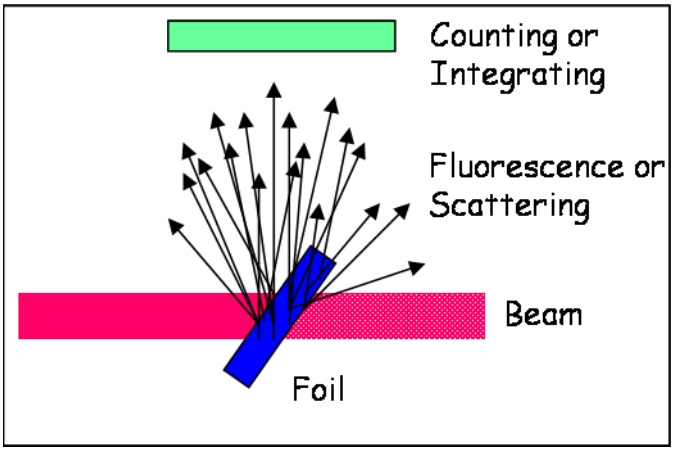

Fig. 13: Principle of an intensity monitor based on beam-induced scattering or fluorescence

3.3.1 Example 1: Intensity measurement set-up used to get the first spectrum at SOLEIL

One of the intensity measurement set-ups installed on the DiffAbs bending magnet BL consists of two 10 µm thick silicon photodiodes procured from Hamamatsu [10]. They are used routinely for the determination of the intensity of the incoming monochromatic beam just before the sample for normalization of the data. Since they are thin, they can be used in parallel with most of the experiments of the BL whose energy range is 3–23 keV, the ‘threshold’ energy being 5 keV for which the transmission is higher than 50%.

DiffAbs was the first beamline opened at SOLEIL and since those devices are sensitive, they were used to get the first spectrum ever measured in the facility, an Extended X-rays Absorption Fine Structure or EXAFS spectrum. A copper foil was inserted between the two photodiodes, under primary vacuum. The experiment consists of a photon energy scan done by the monochromator around an absorption edge of the element which is studied, the K edge of copper in this case. The intensity transmitted by the sample is a function of the linear attenuation coefficient µ:

$$I_1 = I_0 e^{-\mu x}$$

where I_0 and I_1 are the intensities measured on the photodiode located upstream and downstream of the sample, respectively, and x is the thickness of the sample.

The spectrum of Fig. 14 gives the evolution of $\log(I_1 / I_0)$ as a function of the photon energy. The strong change in absorption around 8.97 keV is typical of an absorption edge and appears when photons have enough energy to ionize one electron of the K shell, which is the deepest one. The oscillations observed beyond are characteristic of the short distance order, that is to say the distance between each copper atom and the number of neighbouring atoms.

This spectrum shows that some of the photon beam diagnostics are versatile and can also be employed for achieving the scientific goal of the beamline in addition to the beam conditioning.

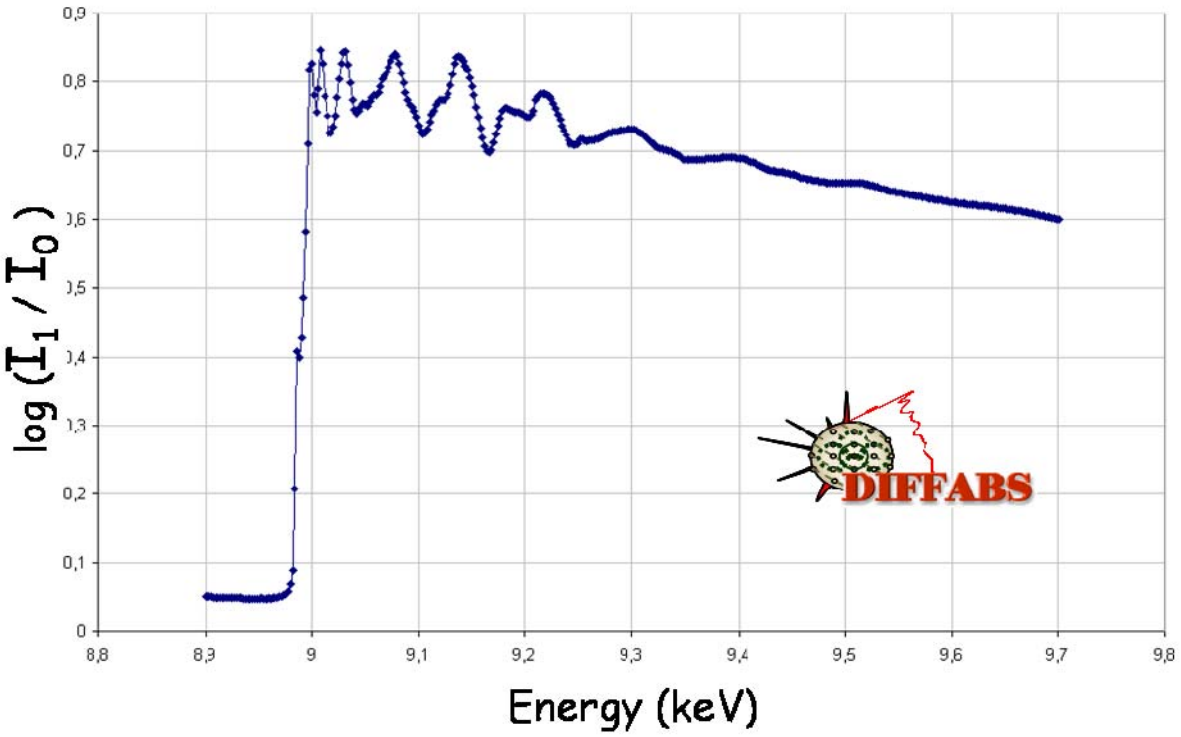

Fig. 14: First Extended X-ray Absorption Fine Structure Spectrum (EXAFS) obtained at SOLEIL DiffAbs, at the copper K edge with two10 µm photodiodes S9724 [10]

3.3.2 Example 2: Combining beam viewing and intensity measurement

The combination of two beam diagnosis techniques can help to a better understanding of the behaviour of the optics and to confirm the theoretical predictions. For instance, on Cristal, a beam viewer and an intensity monitor were used to assess the focusing performances of the monochromator.

The monochromator consists of two crystals (see Fig. 15) and relies on diffraction to select the photons of a given energy or wavelength, following Bragg's law:

$$2d \sin\theta = n\lambda$$

where θ is the diffraction angle, λ is the wavelength of the photons, n is the diffraction order and d is the distance between crystallographic planes in the crystal. The use of two parallel crystals implies that there is only one wavelength propagating horizontally and this enables the energy selection.

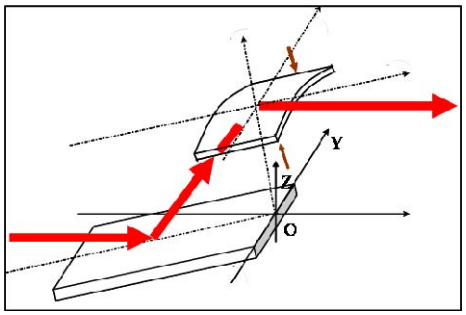

Fig. 15: Principle of a double crystal monochromator for hard X-rays

Figure 16 shows the image of the beam (taken with a device as described in Fig. 9(d)) right after the monochromator, in two different configurations: not focused (left) and focused (right). The focusing occurs when the second crystal of the monochromator is bent. The horizontal size of the beam is then reduced from 1.4 mm down to 0.22 mm and the beam viewer helps to find the bending settings leading to the smallest beam.

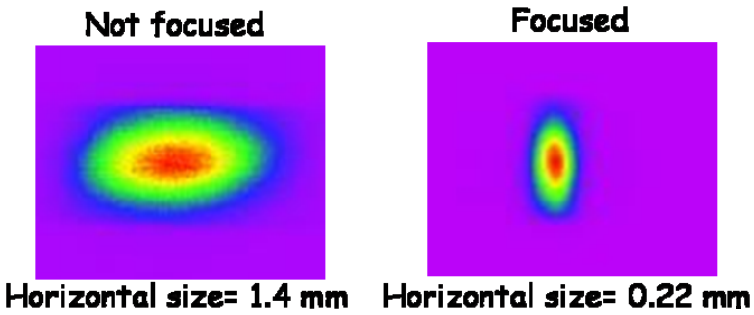

Fig. 16: Images of the beam right after the monochromator in the non-focused (left) and the focused (right) conditions

In a double crystal monochromator, the parallelism of the two crystals has to be optimized to give the best transmission of the selected energy: this is done by measuring a so-called rocking curve, which gives the transmitted intensity as a function of the angle of the second crystal. On the Cristal beamline, the angle is changed by a piezo-motor. Figure 17 show the rocking curves obtained in non-focused mode in black and focused mode in red with an intensity monitor located between the monochromator and the beam viewer. The intensity does not change significantly between the two cases, and the width of the curve, which is related to the resolution of the monochromator is preserved while focusing.

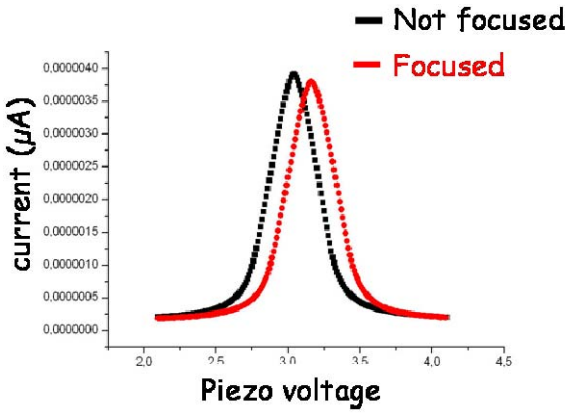

Fig. 17: 'Rocking curves' (see text for explanation) in the non-focused (black) and focused (red) modes

To perform this diagnosis, it was therefore necessary to get an image of the beam to optimize the focus and to measure the intensity of the beam to check that focusing had no significant consequence on the photon flux.

4 An original example of diagnostics: DiagOn

To finish this general presentation of what kind of diagnosis can be performed on the photon beam, I chose to present in detail an original device entirely developed within SOLEIL by the Detectors group, the Optics group, and the Design and Engineering group [11].

In order to reduce the thermal load on the first optical elements of a beamline, it is useful to reduce the collection aperture in the front end to a small angle close to the characteristic divergence of the chosen harmonics. However, photon energy selection not only requires that the undulator be continuously tuned, but also that the aperture be exactly centred on the emission axis, otherwise spectral distortions are observed. The aim of the DiagOn device is to experimentally determine the undulator axis and enable optimal and fast alignment of the adjustable diaphragms of the front-end of each of the VUV and soft X-ray beamlines of SOLEIL.

The spatial distribution of the white beam emitted by an undulator is a broad Gaussian. In the front end, where the apertures have to be placed to protect the optics downstream from incident power, there is no position sensitivity to check the emission axis, as can be seen on Fig.18. This image of the white beam coming out of the first mirror (on the Cassiopée beamline) was obtained with a simple YAG(Ce), at low current in the storage ring, just after the position of the DiagOn, at 20 m from the source. There is no way to localize the emission axis on this picture because there is no position sensitivity.

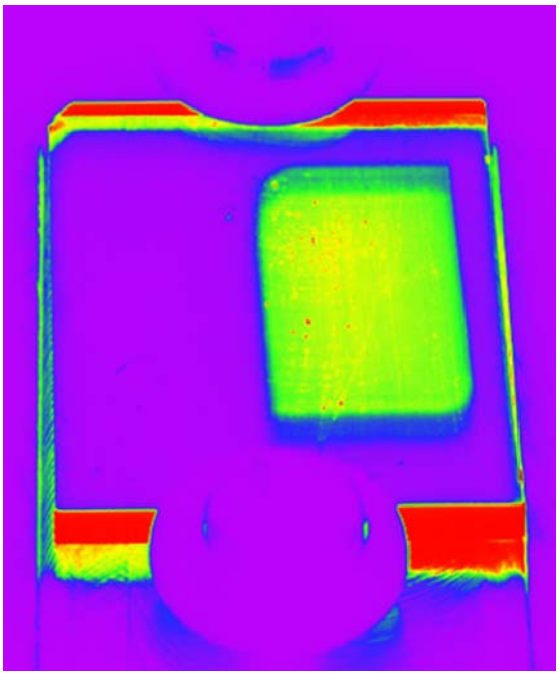

Fig. 18: Image of the pink beam after the first mirror of the Cassiopée beamline with the undulator HU256

The required position sensitivity for the determination of the emission axis (only a few tens of µm) is achieved by spectral filtering in the DiagOn diagnostic itself (Fig. 19). A single wavelength of the white beam is selected by reflection on a multilayer mirror, and directed towards a scintillator.

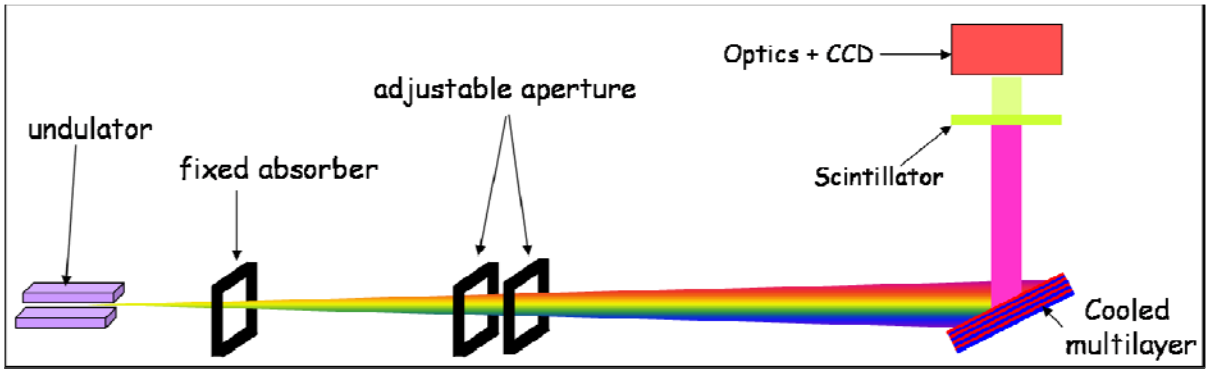

Fig. 19: Schematic description of the operating principle of the DiagOn with the different elements participating in the diagnosis: undulator, adjustable diaphragms and DiagOn; multilayer mirror, fluorescent screen, focusing optics and camera

DiagOn makes use of the undulator's emission properties. In the continuous spectrum emitted, there is a univocal relationship between E, energy of the emitted photons, and θ, their angle of emission with respect to the axis. This relationship appears in the fundamental formula for emission in an insertion device [12]:

$$K^2 = n \times \frac{1900 E_0^2[\mathrm{GeV}]}{\lambda_U[\mathrm{cm}] E[\mathrm{eV}]} - 2\left(1 + \gamma^2 \theta^2[\mathrm{rad}]\right) \quad ,$$

where K is the undulator deflection parameter (which is a function of the magnetic field between the undulator's jaws), n is the harmonic number, E_0 is the electron beam energy, and λ_U is the undulator's period.

For a given K, photons of energy E are emitted on a cone of aperture θ for the n^{th} harmonics of the insertion device, centred on the undulator axis. Consequently, with the selection of one particular wavelength of the emission spectrum, one can extract the corresponding cone. The projection of this cone at the detector position is a ring, whose centre is the emission axis. To get the maximum position sensitivity on the position of the centre, the energy selection has to be performed within a narrow bandwidth, and this can be achieved by a multilayer mirror.

Multilayer coatings are made of alternate reflecting and absorbtion layers of two materials deposited on a silicon substrate. In this application, the thickness of each layer is typically of the order of 1 nm and there are around 50 layers. Multilayer mirrors have a highly chromatic behaviour which follows Bragg's law:

$$n_m \lambda = 2d \sin \theta_m$$

where λ is the reflected wavelength, θ_m is the angle of the reflection, n_m is the order of the reflection and d is the alternation of materials period. Figure 20 shows for instance the reflectivity of a molybdenum–silicon multilayer, with $d = 10$ nm and $\theta_m = 45°$ as a function of the incoming photons' energy. The reflectivity is strongly peaked around 93 eV, providing a strong energy selection, and two other peaks corresponding to the second and third orders of the reflection are also visible but with a much lower intensity.

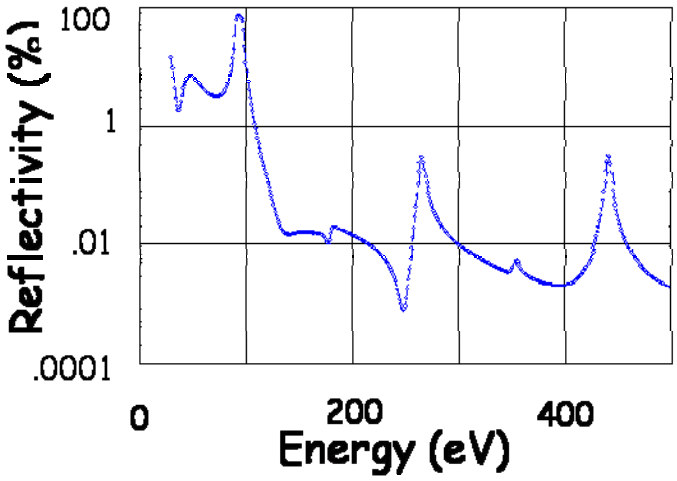

Fig. 20: Reflectivity (%) as a function of incoming photons' energy for a MoSi multilayer with a period of 10 nm at a reflection angle of 45°

This kind of mirror is, of course, a bit delicate, since the layers are really thin. To avoid any interdiffusion or cracking, the temperature of the mirror should be kept below 150°C. Since the DiagOn is a diagnostic for white beam, special care was taken in the mechanical design. The water-cooled holder of the mirror was designed by our Engineering group and the water circulates through microchannels for an improved efficiency.

Figure 21 shows an example of the way the alignment diagnosis is performed, for the Pléïades beamline with the undulator HU80, and a MoB_4C mutilayer mirror reflecting photons at 180 eV. The undulator is first set to a *K* parameter adjusted to get the 180 eV cone at a suitable angle, small enough for 180 eV photons to go through the fixed and adjustable apertures in the front end and large enough for the centre of the circle to be easily found. This position of the centre corresponds to the real optical axis which is materialized on Fig. 21(a) by a red dot. An overexposed image is then taken to observe the shadow of the adjustable aperture and find the centre of the diaphragm [Fig. 21(b)]. A third image, with *K* close to the collapse of the harmonic is also acquired to be able to see a cross [Fig. 21(c)], which was drawn beforehand on the mirror with a diamond point and aligned on the theoretical axis.

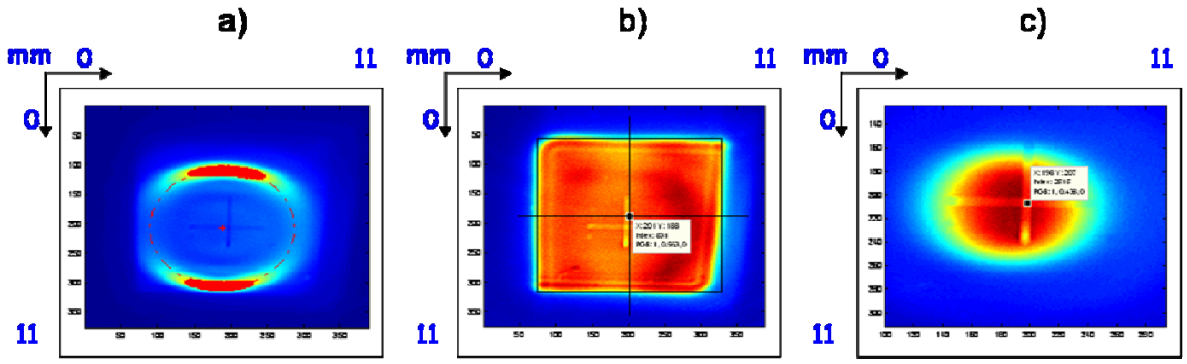

Fig. 21: Steps of the diagnosis with DiagOn on the Pléïades beamline with the HU80 undulator and a MoB_4C multilayer. See text for explanations.

In this example, the theoretical and real axes are shifted by 270 µm horizontally and aligned vertically within the device accuracy. This deviation corresponds to an angular shift of only 13 µrad,

which is acceptable because within the mechanical alignment tolerances. In practice, the adjustable diaphragm is moved to be centred on the real axis and is opened and closed around this position. In case of a strong deviation of the real optical axis, the components of the beamline downstream could be aligned accordingly.

DiagOn has been successfully installed on six SOLEIL beamlines and will be employed on two more and also on two beamlines of the future Spanish synchrotron ALBA.

5 Conclusion

The aim of this lecture was to show that the number of possible diagnoses of a synchrotron photon beam is very important. The examples were chosen to show the variety of devices but they are finally not representative of all the work done throughout the world at synchrotron beamlines to improve their operation and reach ultimate performances. The lecture should therefore be considered only as an introduction to the subject.

The general trend is towards 'on-line' diagnosis, that is to say performed during the experiment itself. There are several reasons for this. For instance, biocrystallography beamlines (but it is also the case in many other fields) cannot fulfil the beamtime demands of their users. The aim foreseen with the improvement of beam diagnostics is the automation of the beamline to improve the sample throughput. Microscopy, or rather, nanoscopy beamlines are strongly emerging. The stability requirements of the optics for these lines are severe, and the need for on-line diagnosis is important either to check that data were acquired in good conditions or to perform feedback on the beamline components.

The final words should therefore be: there is room for innovation and for imaginative people.

Acknowledgements

I would like to thank the organizers of the CAS for offering me the opportunity to give this lecture and J.-C. Denard for suggesting my name. I am very grateful to my colleagues from all the beamlines mentioned in the lecture for providing many of the figures, for their help and their explanations. I also want to thank my colleague K. Medjoubi for his help.

References

[1] FMB, FMB Feinwerk- und Meßtechnik GmbH, now part of Oxford Danfysik, http://www.oxford-danfysik.com/

[2] Bessy Berliner Elektronenspeicherring - Gesellschaft für Synchrotronstrahlung m.b.H, http://www.bessy.de/

[3] K. Holldack *et al.*, 5th European Workshop on Diagnostics and Beam Instrumentation for Particle Accelerators, DIPAC 2001, Grenoble, 2001, pp. 16–20.

[4] K. Holldack *et al.*, *Nucl. Instrum. Methods Phys. Res.* **A467** (2001) 213.

[5] IRD, International Radiation Detectors Inc., http://www.ird-inc.com/

[6] Saint Gobain Solcera, http://www.solcera.com/

[7] R. Tucoulou *et al.*, *J. Sync. Rad.* **15** (2008) 392.

[8] Baikowski, http://www.baikowski.com/fr/technical_markets/tm_ceramicYAG.shtml

[9] F. Senf *et al.*, *Nucl. Instrum. Method Phys. Res.* **A467** (2001) 474.

[10] S9724 photodiodes from Hamamatsu, http://www.hamamatsu.com/

[11] K. Desjardins *et al.*, proceedings of *IEEE Nuclear Science Symposium 2008*, to be published.

[12] K.-J. Kim, *Nucl. Instrum. Methods Phys. Res.* **A246** (1986) 67.